MeMeA 2009 - International Workshop on Medical Measurements and Applications
Cetraro, Italy
May 29-30, 2009

Rectangular Wave Excitation in Wideband Bioimpedance Spectroscopy

Mart Min, Toivo Paavle, Paul Annus, and Raul Land
Department of Electronics
Tallinn University of Technology
Tallinn, Estonia
e-mail: min@elin.ttu.ee

Abstract— **Method of time domain impedance spectroscopy using of rectangular wave chirp excitation is presented in the paper. Effectiveness of the excitation is high – more than 85% of the generated energy lies in the useful excitation bandwidth, which can cover several decades of frequency. Fast measurement and joint time-frequency analysis of dynamic impedances is envisaged. Implementations in impedance spectroscopy for cell detection and characterizing in different lab-on-a-chip type high-throughput microfluidic devices can be one recommended area for the proposed method. This method offers important diagnostic information about the dynamic and structural properties of biological cells, organs like beating heart, and the whole cardiovascular system.**

Keywords- impedance spectroscopy; bioimpedance; signum-chirp; rectangular chirp; bidirectional chirp; maximum length sequence; cross-correlation; Fourier analysis.

I. INTRODUCTION

Frequency domain impedance measurement is still a common approach in assessing passive electrical properties of cells and tissues [1]. However, sweeping or hopping of a sine wave excitation over a wide frequency range is too slow for performing impedance spectroscopy to recover fast impedance changes in biological objects as single cells and cell cultures moving in high throughput microfluidic devices [2-5]. The use of short-time but broadband pulse excitation and monitoring the response as a function of time will greatly reduce the measurement interval. The sine wave based chirp excitation – a non-periodic one-shot signal with continuously changing frequency – has been found to be the most promising in terms of its well defined frequency range, acceptable crest factor, and achievable signal-to-noise ratio [6].

Signal processing is much simpler when the rectangular wave excitation with only +1 and −1 value is used. Moreover, the rectangular wave forms have the minimal crest factor (equal to 1). A known method is to generate a pseudo-random maximum length sequence (MLS) of rectangular pulses [4, 5]. In the paper, there is proposed another method – generation of a sequence of regularly shortening or widening rectangular pulses. In this case we have a rectangular chirp excitation, which can be described as a signum-chirp function instead of the sine chirp [7, 8]. Besides the simplest rectangular chirp having non-return-to-zero (NRZ) pulses (zero-states are absent), some versions of return-to-zero (RZ) rectangular chirp function (has +1, 0, and −1 values) are considered [9] and compared.

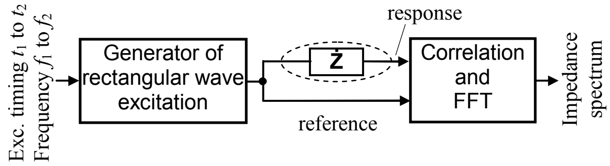

Figure 1. Basic structure of the measurement system.

Fig. 1 depicts a simplified impedance analyzer, in which the rectangular wave excitation is generated during the excitation time interval T_{exc} from t_1 to t_2, which covers a pre-selected excitation bandwidth B_{exc} from f_1 to f_2. The excitation passes the impedance Ż and gives a response, which will be cross-correlated with a reference pulses (the same signal as excitation, typically). The result is a time domain correlation function representing an impulse response $g(t)$ of the complex impedance Ż. Performing the Fourier transform, we will obtain a complex impedance spectrum $S(j\omega)$ or frequency responses of magnitude $M(\omega)$ and phase $\varphi(\omega)$ separately.

II. RECTANGULAR WAVE SIGNALS

Four types of rectangular excitation signals, being under the analysis, are shown in Fig. 2, and characterized below. The signals were generated with duration T_{exc}=10 ms, but for better visualization only the initial segments of pulses are shown.

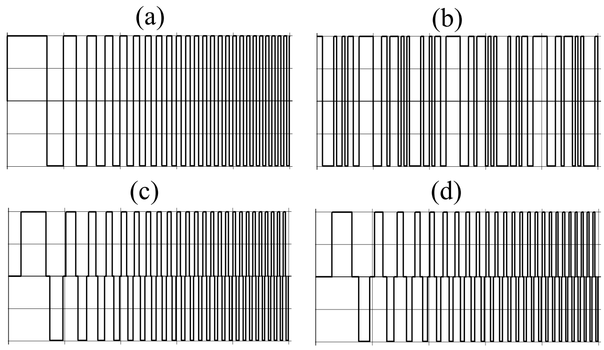

Figure 2. Excitation waveforms ($V(t)$): (a) signum-chirp, NRZ pulses, zero-state is absent; (b) 7-stage MLS; (c) rectangular chirp, 18° zero-state RZ pulses; (d) rectangular chirp, 30° zero-state RZ pulses.

- signum-chirp (pseudo chirp) with initial and final frequencies of f_1=1 Hz, and f_2=100 kHz (useful excitation bandwidth $B_{exc}=f_1–f_2=10^5$ Hz). The signal is generated at a sampling rate f_s=1.5 Msamp/s (Fig. 2a).

978-1-4244-3599-9/09/$25.00 ©2009 IEEE

- 7-stage maximum length sequence (MLS) with a clock rate $f_c = f_s/15 = 100$ kHz and sequence period $T_{seq} = T_{MLS} = (2^7-1)/f_c = 1.27$ ms. The MLS spectrum reaches zero level at $f = B_{MLS} = 100$ kHz (see Fig. 2b and Fig. 4).
- rectangular chirp with return-to-zero (RZ) pulse waveform: zero-state 18° per a quarter of "period" (in fact, chirp is not periodic). The same parameters are used as in case 1, only f_s = 5 Msamp/s (Fig. 2c).
- rectangular chirp, the same parameters as in previous case, only the zero-state is widened to 30° (Fig. 2d).

III. Excitation Energy of Signals

The Fast Fourier transform (FFT) up to $max\,f$=750 kHz with frequency resolution Δf=100 Hz was used for energy analysis. The results and following illustrations are obtained by means of a specially developed PC simulator, which bases on the structure, shown in Fig. 1.

A. Signum-chirp

The waveform of a linear signum-chirp is shown in Fig. 2a, and the amplitude spectrum of the respective pulse is shown in Fig. 3.

Energy of the rectangular chirp signal $V_{ch}(t)$ with amplitude A can be expressed in time domain as follows:

$$E_{ch} = \int_{t_1}^{t_2} \left|V_{ch}(t)\right|^2 dt = A^2 T_{exc} \tag{1}$$

According to Parseval's theorem, the total energy in the frequency domain must be the same as calculated from (1) in time domain. Due to the rectangular waveform which contains higher frequency harmonic components [10], certain part of the signal energy E_{out} falls outside the excitation bandwidth B_{exc}.

The fundamental harmonic with the amplitude $A_0 = (4/\pi)A$, RMS value $A_0/\sqrt{2} = \left(4/\pi\sqrt{2}\right)A$, energy $E_1 = (A_0^2/2)\,T_{exc} = (8/\pi^2)\,A^2 T_{exc}$, and power $W_1 = E_1/T_{exc} = (8/\pi^2)\,A^2$, creates a constant value power spectral density (PSD) $w_1 = W_1/B_{exc}$, V^2/Hz, within the bandwidth B_{exc}:

$$w_1 = \left(8/\pi^2\right) A^2 / B_{exc} \tag{2}$$

The power of every k-th higher odd harmonic (k=3, 5, 7, …) is equal to W_1/k^2, being spread over the range $kf_2 - kf_1 = kB_{exc}$. The PSD for higher harmonics can be expressed as $w_k = (w_1/k^2)/k = w_1/k^3$.

The total power of the signal $V_{ch}(t)$ is gradually distributed over the whole frequency range – see Fig. 3. The PSD p_L of every gradual L-th level (L= 1, 2, 3, 4, 5, …) of the spectrum, beginning from the first one p_1, is the sum of power spectral densities of the fundamental w_1 and higher harmonics w_k contributing into the given level L. Into the PSD p_1 contribute all the signal components $p_1 = w_1 + w_3 + w_5 + w_7 + \ldots$, but into the next level mere the higher harmonics (k=3, 5, 7, …), $p_2 = w_3 + w_5 + w_7 + \ldots$, into the third level only the harmonics beginning from k=5, $p_3 = w_5 + w_7 + \ldots$, etc.

Generally

$$p_L \approx w_1 \sum_{i=L}^{\max L} (2i-1)^{-3}\,, \tag{3}$$

with max$L \to \infty$ in the theoretical consideration (i= 1, 2, 3, …).

The partial power $P_1 = p_1 B_{exc}$ of the main bandwidth of chirp (useful power) is P_{exc}, while the power falling outside of it, P_{out}, is the summed up power of the next stage

$$P_{out} \approx W_1 \sum_{i=1}^{\max L} 2(i-1)/(2i-1)^3\,. \tag{4}$$

As the minimal frequency for every level is kf_1, then the equations (3) and (4) are approximate ones and the equalities are exact only for f_1=0. When the excitation bandwidth B_{exc} exceeds one decade ($f_2/f_1 > 10$), these equations are exact enough for engineering calculations.

The chirp energy $E_{ch} = E_{exc} + E_{out} = (P_{exc} + P_{out})\,T_{exc}$ and the useful excitation energy $E_{exc} = P_{exc}\,T_{exc}$. From (3) and (4) follows the role of useful energy $\delta_E = E_{exc}/E_{ch}$, and considering f_1=0, it can be derived from (3) and (4) as

$$\delta_E = \left(\sum_{i=1}^{\max L} (2i-1)^{-3}\right) \Big/ \left(\sum_{i=1}^{\max L} (2i-1)^{-2}\right) \tag{5}$$

For max$L \to \infty$, the sums in (5) can be expressed via Riemann zeta function $\zeta(x) = \sum_{n=1}^{\infty} n^{-x}$. It is known from mathematics that the sum $\sum_{i=1}^{\infty} (2i-1)^{-2} = \pi^2/8$, and $\sum_{i=1}^{\infty} (2i-1)^{-3} = 7\zeta(3)/8$, where $\zeta(3) \approx 1.202$ is termed as the Apéry's constant [11]. Now, using these equalities, we can express the percentage of useful energy in the linear NRZ signum-chirp pulse as

$$\delta_E = 7\zeta(3)/\pi^2 \tag{6}$$

At max$L$ >>1, the $\delta_E \approx 0.85$ and the spectrum has almost uniform energy distribution over the B_{exc}. In simulations δ_E=(0.84…0.88) was obtained depending on the simulation methods and parameters used. The relative decrement of every L-th step of magnitude can be calculated from (3) as $\delta_L = (E_{exc}/E_L)^{1/2} = A_1/A_L$. The values for some lower order levels are $\delta_2 \approx 4.51$, $\delta_3 \approx 8.44$, and $\delta_4 \approx 12.47$ – see approximation in Fig. 3. For the next levels, the values of $\delta_L \approx 4(L-1)+1$ are roughly valid.

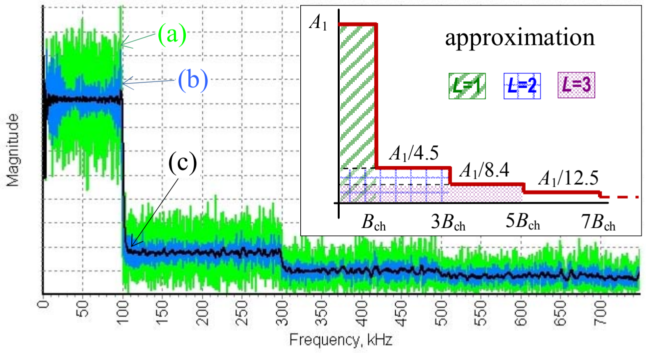

Figure 3. Amplitude spectrum of signum-chirp: (a) without averaging; (b) with 4-tap moving averaging; (c) with 32-tap moving averaging.

B. *Maximum Length Sequence*

The spectrum of MLS has a sinc-function type envelope (Fig. 4), about 90% of total energy E_{MLS} lies in the 0 to 100 kHz range ($B_{\mathrm{MLS}}=f_s$) [4]. We cannot use all the B_{MLS} range for excitation, because the spectral density goes down with frequency and reaches zero at the end of B_{MLS} (100 kHz). A reasonable frequency limit is 44 kHz, at which the RMS spectral density reduces to –3 dB level (density of power spectrum reduces to 0.5 level). In this case we can use about 70% of the B_{MLS} range energy for excitation. It means that about 63% of total energy generated by the MLS signal (E_{MLS}), can be used for excitation, $E_{\mathrm{BW}} \approx 0.7(0.9E_{\mathrm{MLS}}) = 0.63E_{\mathrm{MLS}}$.

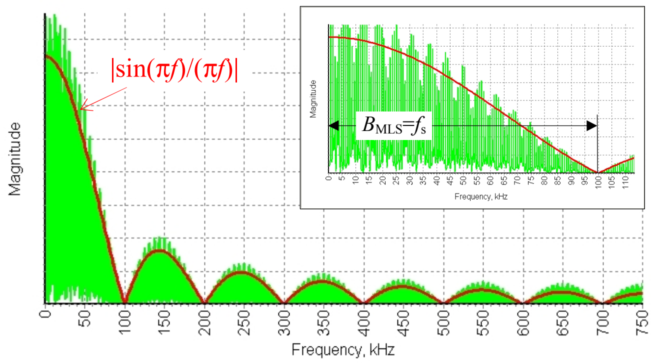

Figure 4. Amplitude spectrum of 7-stage MLS.

C. *Shortened pulse rectangular chirps*

The waveforms of shortened pulse rectangular chirps (three-level RZ chirp pulses) are shown in Figs. 2c and 2d. To follow the Nyquist rule, the sampling rate for generation RZ pulses must be higher than for the respective NRZ pulse. The results in Fig. 5 are obtained with f_s= 5 Msamp/s, which yields $max\, f$=2500 kHz and Δf=100 Hz at the direct FFT processing of signals. Two cases, with 18° and 30° shortening modifications are considered.

a) 18° zero-level state (the 5th “harmonic” is removed [9]). Minimal sampling rate is min f_s=2·(360/18)f_2=40f_2. The total generated energy $E_{18} = 0.8E_{\mathrm{ch}}$, and $E_{\mathrm{exc}} > 0.9E_{18}$. This is still the best result – less than 10% of energy falls outside the excitation BW.

b) 30° zero-level state (the 3rd “harmonic” is removed [9]). Minimal sampling rate is min f_s=2·(360/30)f_2=24f_2. The total energy is $E_{30} = 0.67E_{\mathrm{ch}}$, and the part of useful excitation energy is about 90% ($E_{\mathrm{exc}} \leq 0.9E_{30}$). The result is acceptable, but slightly worse than in previous case (a), related to 18° zero-level state.

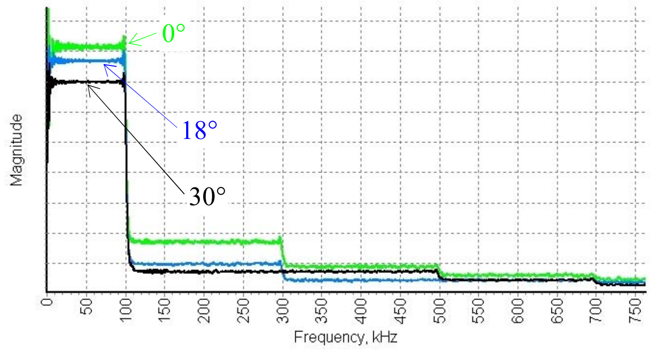

Figure 5. Amplitude spectra of the three-level RZ rectangular chirps (32-taps moving averaging has been applied).

D. *Bidirectional signum-chirp*

To eliminate the impact of the unavoidable DC component of chirp pulses, the bidirectional chirps can be used, i.e., two sequental mirrored chirp pulses with frequency sweep from f_1 to f_2, and f_2 to f_1, respectively, are generated (see the next chapter). In this case, the energy distribution is similar to the corresponding unidirectional chirp.

IV. Simulation Examples

A. *Time domain*

In Fig. 6, examples of bidirectional signum-chirp excitation chirp at sweep rate of ±40 kHz/s are shown. Let us pay attention to the trailing ends of response signal V_{rsp}, which must be considered to gain perfect results at selection of the observation time for the following cross-corrrelation.

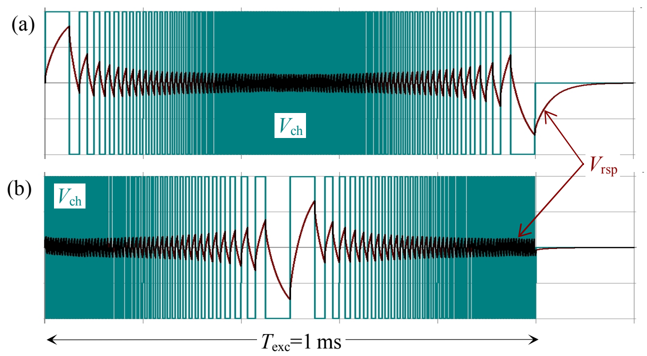

Figure 6. Bidirectional chirp excitation and response : (a) up chirping f_1=0, f_2=200 kHz; (b) down chirping f_1=200 kHz, f_2=0.

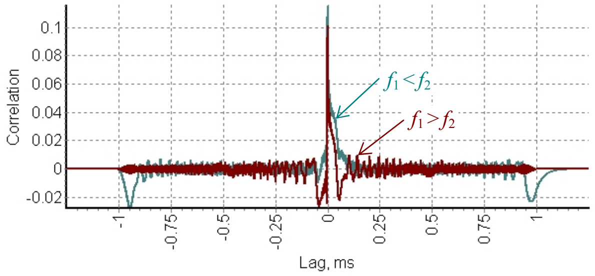

Figure 7. Cross-correlation between bidirectional chirp excitation: up chirping ($f_1 < f_2$) and down chirping ($f_1 > f_2$) correlation products.

B. Cross-correlation

In Fig. 7, cross-correlation functions (CCF) between the bidirectional signum-chirp excitation with T_{exc}=1 ms and the respective response are shown (see previous example). The CCF is evaluated from lag $\tau = -1.25$ ms to $+1.25$ ms with minimal possible lag step $\Delta\tau = 1/f_s$ and it includes all the information about impedance vector under study over the whole excitation bandwidth.

C. Spectral analysis

In the proposed solution for wideband (bio)impedance spectroscopy the array of CCF values is used as the input sequence for the FFT processing. It bases on the fact that in accordance with the cross-correlation theorem (generalized Wiener-Khinchin theorem), the correlation function is equivalent to the inverse Fourier transform of the cross-power spectral density [12].

As the result, we obtain the real and imaginary parts of the impedance, from which obtaining of the amplitude and phase response is an ordinary procedure. Thereby, for interpreting the results, the phase response should be preferred because of its minor dependence on all kind of fluctuations. The phase response $\varphi(\omega)$=arctg [Im(ω)/Re(ω)] characterizes relative variations of the relationship between imaginary Im(ω) and real part Re(ω). The phase response is of great diagnostic value – it does not depend on magnitude and common disturbances. The phase curves in Fig.8 can be interpreted as reducing of ischemia connected with decreasing of the extracellular resistance from its initial value R_{ext}, e.g., as a result of reperfusion after transplantation of a muscle flap.

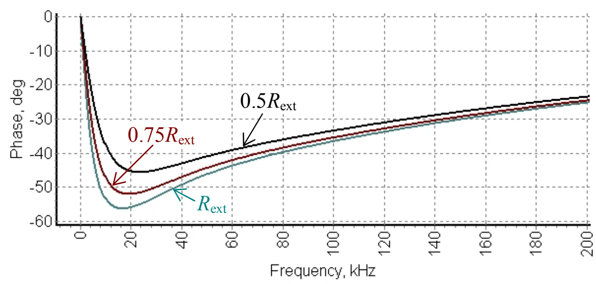

Figure 8. Phase spectrum at different values of extracellular resistance R_{ext} (frequency resolution Δf= 400 Hz).

V. Conclusion

Rectangular wave signum-chirps are rather effective in wideband impedance spectroscopy. More than 85% of the generated energy becomes useful for excitation when using NRZ pulses. Modifications like introducing of RZ pulses can enhance the percentage of effectiveness over 90%. In comparison, the MLS contains only 63% of energy usable for excitation.

Bidirectional chirp excitation (up- and down-chirping) avoids the DC component. Furthermore, first down- and then up-chirping has a clear advantage – the transient response is much shorter than in opposite case.

Acknowledgment

This research was supported by the European Union through the European Regional Development Fund, Estonian Science Foundation, grants no. 7212 and 7243, and Enterprise Estonia through ELIKO Competence Center.

References

[1] S. Grimnes, and Ø. G. Martinsen, Bioimpedance and Bioelectricity Basics (2nd ed.), Elsevier-Academic Press, 2008.

[2] T. Sun, C. van Berkel, N. G. Green, and H. Morgan, Digital signal processing methods for impedance microfluidic cytometry, Microfluid Nanofluid, vol. 6, No. 2, Feb., 2009, pp. 180-187.

[3] T. Sun, S. Gawad, C. Bernabini, N. G. Green, and H. Morgan, "Broadband single cell impedance spectroscopy using maximum length sequences: theoretical analysis and practical considerations", Meas. Sci. Technol. **18** (2007), 2859–2868, IOP Publishing, 2007.

[4] S. Gavad, T. Sun, N. G. Green, and H. Morgan, Impedance Spectroscopy Using Maximum Length Sequences: Application to Single Cell Analysis, Review of Scientific Instruments, **78**, 054301-1, American Institute of Physics, 2007.

[5] T. Sun, D. Holmes, S. Gawad, N. G. Green, and H. Morgan, "High speed multi-frequency impedance analysis of single in a microfluidic cytometer using maximum length sequences", Lab Chip, 2007, **7**, pp. 1034–1040.

[6] M. Min, U. Pliquett, T. Nacke, A. Barthel, P. Annus, and R. Land, "Broadband excitation for short-time impedance spectroscopy", Physiol. Meas. **29** (2008), S185-S192. DOI: 10.1088/0967-3334/29/6/S16.

[7] T. Paavle, M. Min, T. Parve, "Using of chirp excitation for bioimpedance estimation: theoretical aspects and modeling", Proc. of the Baltic Electronic Conf. BEC2008, Oct. 6-8, 2008, Tallinn, Estonia, pp. 325-328.

[8] M. Min, "Embedded signal processing in impedance spectroscopy", Norchip2008, 6 pp., available digitally in IEEE Xplore.

[9] M. Min, T. Parve, "Improvement of lock-in electrical bio-impedance analyzer for implantable medical devices", IEEE Trans. IM, **56**(3), 2007, pp. 968-974.

[10] M. Pollakowski, H. Ermert, "Chirp signal matching and signal power optimization in pulse echo mode ultrasonic nondestructive testing", IEEE Trans. on Ultrasonics, Ferroelectrics, and Frequency Control, **41**(5), 1994, pp. 655-659.

[11] H. B. Dwight, Tables of Integrals and Other Mathematical Data (4th ed.), The MacMillan Company, New York, 1961.

[12] S. V. Vaseghi, Advanced Digital Signal Processing and Noise Reduction, John Wiley & Sons Ltd, Chichester, England, 2006.